Journal of Statistical Physics, Vol. 49, Nos. 1/2, 1987

Nonequilibrium Discontinuous Phase Transitions in a Fast Ionic Conductor Model: Coexistence and Spinodal Lines

J. Marro[1,2] **and J. L. Vallés**[1,3]

Received December 17, 1986; revision April 7, 1987

Two-dimensional lattice-gas models with attractive interactions and particle-conserving hopping dynamics under the influence of a very large external electric field along a principal axis are studied in the case of off-critical densities. We describe the corresponding nonequilibrium first-order phase transitions, evaluate coexistence and spinodal lines, and make some comparisons with experimental observations on fast ionic conductors.

KEY WORDS: Stochastic lattice-gas model; stationary nonequilibrium states; fast ionic conductors; metastability; nonequilibrium first-order phase transitions.

1. INTRODUCTION

Several versions of the Ising model, including the so-called fast ionic conductor model, have been used during the recent past in the analysis of stationary nonequilibrium states.[4] The fast ionic conductor model is a lattice-gas version of the Ising model, where ions are located at lattice sites and interact via a nearest neighbor pair potential J, provided with a stochastic dynamics consisting of jumps to neighboring unoccupied sites under the influence of both a thermal reservoir at temperature T and a uniform external electric field E. In the absence of the latter ($E=0$), the transition rates are such that the stationary state of the system is the Gibbs equilibrium state at the reservoir temperature T. However, a uniform field E along one of the principal directions of the lattice, say $\hat{x}$, which forms a

---

[1] Departamento de Física Fonamental, Universitat de Barcelona, E-08028 Barcelona, Spain.

[2] Present address: Courant Institute of Mathematical Sciences, New York University, 251 Mercer Street, New York, New York 10012.

[3] Departamento de Física, Facultad de Ciencias, Universidad de Granada, Granada, Spain.

[4] See Ref. 1 (henceforth referred to as II) for references.

closed loop, e.g., by assuming a lattice with periodic boundary conditions, biases the jumps in the direction $\hat{x}$ and produces a net steady current of ions in the system; the (stochastic) interaction with the reservoir then maintains a steady nonequilibrium condition by dissipating the heat generated by the current.

Previous studies on that model, e.g., in the case of a saturation field $E \rightarrow \infty$,(1) demonstrated the existence of a second-order or continuous phase transition at a certain critical temperature T_c^* when the lattice is half-filled with particles or ions. They also revealed that, while the phase segregation when $E=0$ occurs into randomly oriented regions below T_c, the equilibrium critical temperature, the nonequilibrium states for $E \neq 0$, are highly anisotropic, e.g., they consist below T_c^* of two dimensions of a fluid or particle-rich phase whose particles are clustered into a single strip parallel to the direction $\hat{x}$, coexisting with a gas or particle-poor phase filling homogeneously the rest of the system. Moreover, it was found that $T_c^* > T_c$ for $J > 0$ (i.e., attractive interactions between particles), that $T_c^* < T_c$ for $J < 0$ (repulsive), and that there is a sudden break in the slope of the current versus temperature curve at T_c^*.(1)

These and other reported features of the models seem to characterize essentially a class of materials having promising technological applications, namely solid electrolytes capable of relatively large ionic conductivities below the melting point.(2–5) When making comparisons with related experimental observations, however, one needs to concentrate on the most appropriate versions of the idealized models. Accordingly, we consider in this paper the case of a two-dimensional fast ionic conductor model with attractive interactions and very large external electric field when the particle density is smaller than critical, the case considered in II; the model system in the present case undergoes a first-order or discontinuous phase transition very similar to the one shown by most real materials. In addition to some sensible comparisons with experimental results, our model then allows the evaluation of coexistence and spinodal lines, and the study of the corresponding system relaxation showing the existence of metastable states that are very different in nature from the intermediate multi-strip states reported in II for half-filled lattices. The fact that we restrict ourselves here to the two-dimensinal case is also favorable when trying to interpret experimental observations in the light of the behavior of the model, given that solid electrolytes sometimes present low dimensionality effects, as we shall discuss later. On the contrary, our restriction to the case $J > 0$ was motivated by simplicity and by the fact that the phase transition seems to be suppressed in the presence of the external electric field for $J < 0$ in some cases(1) (also, $J > 0$ is more suitable for a Monte Carlo analysis).

2. SYSTEM EVOLUTION AND METASTABILITY

The model system of interest here is precisely the one described in II, except that the system density,

$$\rho = N^{-1} \sum_i n_i \tag{2.1}$$

where $N = L^2$ and $n_i = 1$ (ion) or 0 (hole), is the occupation variable at each lattice site $i = 1, \ldots, N$, and is allowed to have values differing from the critical one, $\rho = 1/2$; we thus refer to II for most details and definitions and for the relevant bibliography. In the present case we report on computer simulations for $\rho = 0.05$, 0.075, 0.1, 0.2, and 0.35 at several temperatures, which complement the case $\rho = 0.5$ considered in II. The computations refer to lattices $L = 50$ and 100; our conclusions here seem mostly independent of finite-size effects.

The initial configuration for each experiment was, unless otherwise indicated, the one corresponding to infinite temperature, i.e., random distribution of ρN particles over the N lattice sites. The evolutions then lasted until the distributions of values for the order parameter $m(T)$ and for the configurational energy $u(T)$, both quantities defined in II, approached good Gaussians (excluding the values corresponding to the initial transient regime); this required typically between 10^5 and 10^6 Monte Carlo steps.

As in the case $\rho = 1/2$, when the system with $\rho < 1/2$ is quenched below the coexistence curve, say below some temperature $T^*(\rho)$, the system is seen to segregate into two phases, the liquid phase being highly anisotropic under the influence of the infinite external electric field. This shows up, for instance, in the presence of striplike configurations below $T^*(\rho)$ such as those in Fig. 1. The configurations above $T^*(\rho)$ also reveal typically some ordering (cf. Fig. 1), namely anisotropic clusters preferentially directed along the field direction, an effect discussed in some detail in II.

During the evolutions at $\rho = 0.35$ below $T^*(\rho)$, the systems with $L = 50$ first segregate, as was the case for $\rho = 1/2$ in II, into two rather compact strips along the field direction, which then finally coalesce during our evolutions to form the expected one-strip stationary states; see Fig. 2. When $\rho \leqslant 0.2$, on the contrary, there are not enough particles in the system to build up those intermediate states, and the evolution most often proceeds directly through one-strip states, which become more and more compact with time.

In addition to the above intermediate multistrip states, the system with $\rho < 1/2$ presents well-defined metastable states. These are quite evident in the case $\rho \leqslant 0.2$, as depicted, for instance, in Fig. 3.

We would like to emphasize at this point the very different nature shown by the intermediate multistrip states, as in Fig. 2, and by the real

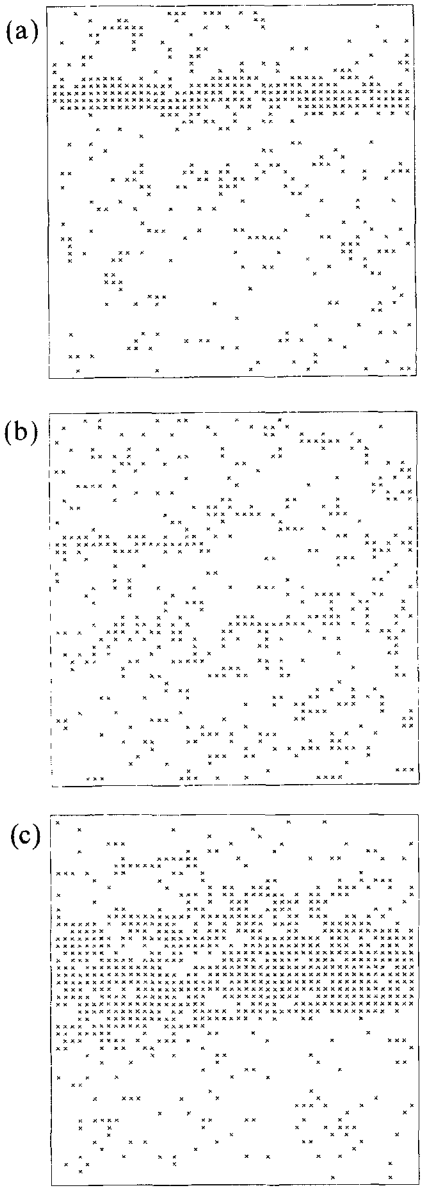

Fig. 1. Typical configurations during the stationary regime in the case of a lattice $L=50$ with periodic boundary conditions under the influence of an infinite external electric field along the horizontal direction. (a) $\rho=0.2$ and $T=1.13T_c<T^*(\rho)$, where T_c represents the equilibrium (Onsager) critical temperature. (b) $\rho=0.2$ and $T=1.2T_c>T^*(\rho)$. (c) $\rho=0.35$ and $T=1.2T_c<T^*(\rho)$. (d) $\rho=0.35$ and $T=1.4T_c>T^*(\rho)$.

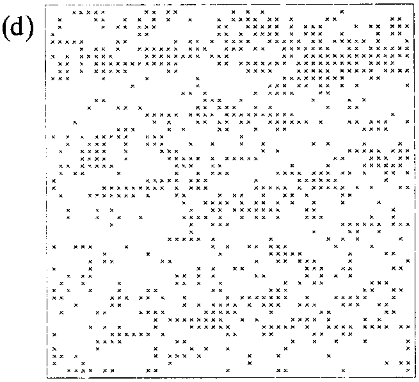

Fig. 1 (*continued*)

metastable states revealed by Fig. 3. The former might be termed metastable in the sense that they satisfy the criterion introduced by Binder and Müller-Krumbhaar.(6) That is, given a relaxing macroscopic quantity A, one may define the relaxation function

$$\Phi_A = \frac{A(t) - A(\infty)}{A(0) - A(\infty)} \tag{2.2}$$

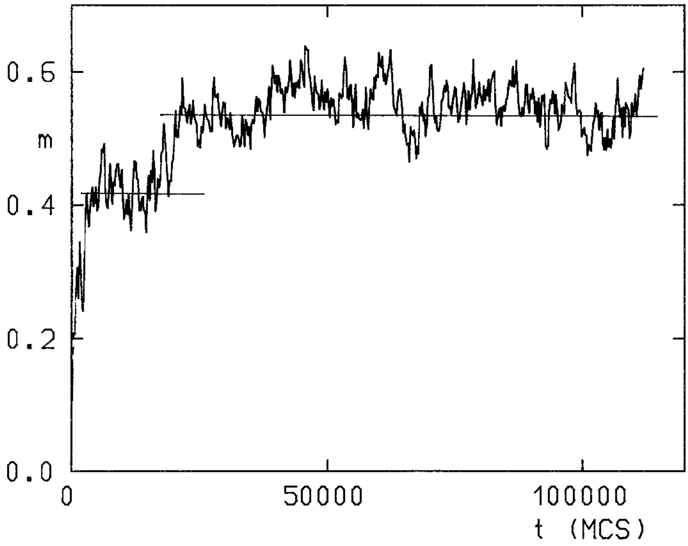

Fig. 2. Evolution of the order parameter in the case $L = 50$, $\rho = 0.35$, and $T = 1.25T_c$. One observes the abrupt relaxation of the system from an intermediate, segregated two-strip state to the final, stationary one-strip state.

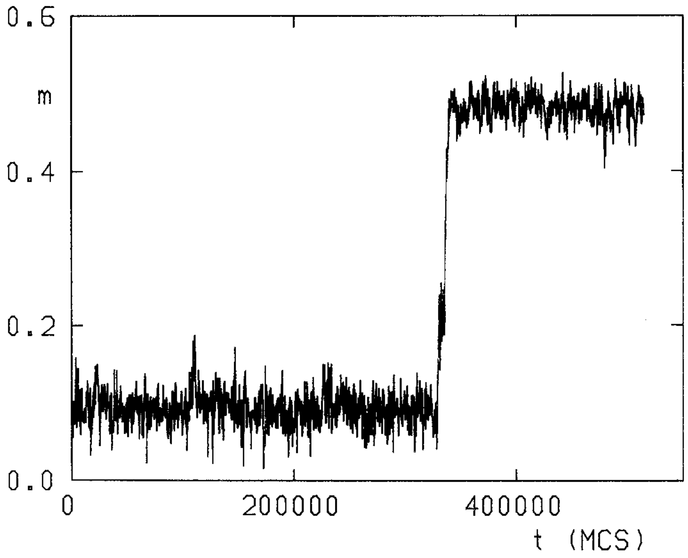

Fig. 3. Evolution of the order parameter in the case $L=50$, $\rho=0.1$, and $T=0.8T_c$. One observes the abrupt relaxation of the system from a real, metastable, nonsegregated state to the final one-strip segregated state.

and the associated relaxation time

$$\tau_A=\int_0^\infty dt\, \Phi_A(t) \tag{2.3}$$

A metastable state is then characterized by the absence of a noticeable evolution on a macroscopically large enough time scale and, consequently, by the presence of a plateau in the function $\Phi_A(t)$. This is certainly the case when A represents, for instance, the order parameter or the configurational energy during evolutions with intermediate states such as the one represented in Fig. 2. Actually, the lifetime of those intermediate states increases with decreasing temperature and, as reported in II, it was observed to practically diverge in some cases for $\rho=1/2$.

The fact that multistrip states are not real, metastable, however, follows immediately by considering the three properties listed by Penrose and Lebowitz(7) characterizing metastable states: (i) only one thermodynamic phase is present (and usual thermodynamics applies to it); (ii) an (isolated) system that starts in this state is likely to take a very long time, say years, to get out; and (iii) escape from the metastable state is an irreversible process. The two-strip states reported for $L=50$ certainly accomplish (ii), as noticed in the previous paragraph, and (iii); actually, we never observed reversibility for $\rho \leqslant 1/2$. However, they are segregated states, thus violating (i). Even more, their nature is size-dependent in the sense that, as clearly observed for $\rho = 1/2$, the number of strips in the longest lived intermediate multistrip state increases with L, and $\Phi_A(t)$ evolves in those cases via several abrupt steps. On the contrary, states such as the one reported in Fig. 3 for $t \leqslant 3 \times 10^5$ MC steps are metastable according to all the above criteria. In any case, it should be remarked that both multistrip and metastable states are in this case a nonequilibrium effect, and that the former do not seem to have an equilibrium counterpart.

3. COEXISTENCE AND SPINODAL LINES

Another distinct feature of the case $\rho < 1/2$, as compared to that of a critical density in II, is depicted by the histograms in Fig. 4. That is, when $\rho < 1/2$ there is no symmetry around $L\rho$ and, in particular, the longitudinal case presents two different peaks [the small one almost imperceptible in Fig. 4 because it corresponds to $T \lesssim T^*(\rho)$, so that the strip configuration is not very compact].

A more quantitative picture of the anisotropic phase segregation can be obtained from the behavior with ρ and T of the order parameter,

$$m(\rho) = \tfrac{1}{2}[\rho(1-\rho)]^{-1/2}\,[\langle M_x^2 \rangle_T - \langle M_y^2 \rangle_T]^{1/2} \tag{3.1}$$

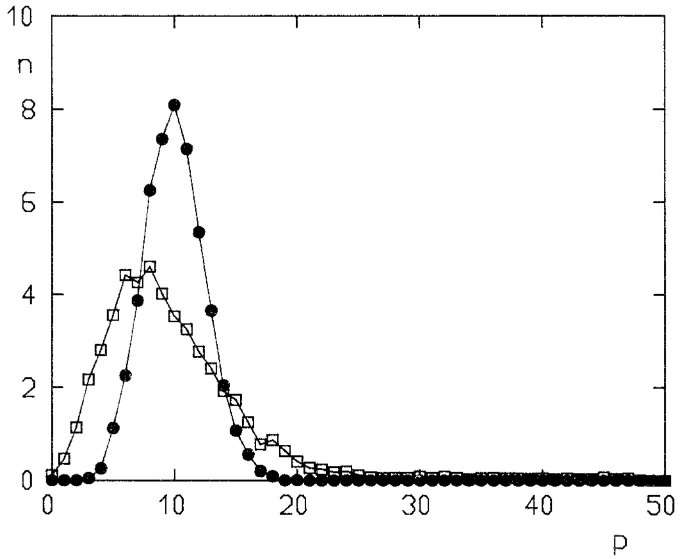

Fig. 4. Number of columns (□) in the direction of the field and (●) in the direction perpendicular to the having $p = 0, 1, \ldots, L-1$ particles, versus p in the case $\rho = 0.2$ and $T = 1.15T_c$.

where M_x^2 and M_y^2 represent, respectively, the squared longitudinal and transverse magnetizations defined in II. As shown by Fig. 5, $m(\rho)$ as a function of temperature follows in the case $\rho = 0.35$ a continuous trend quite similar to the one for $\rho = 1/2$, while it presents for $\rho \leqslant 0.2$ a discontinuity at a temperature $T^*(\rho)$ associated with the previously reported metastable states near $T^*(\rho)$. The situation is clearly that of a first-order or discontinuous phase transition for $\rho \leqslant 0.2$, this probably being too weak at $\rho = 0.35$ to be evidenced by our data. This seems confirmed by the data we report in Section 4.

Table I lists the values we finally evaluated for the transition temperature $T^*(\rho)$, $T_c^* \equiv T^*(\rho = 1/2)$ corresponding to the critical temperature characterizing the second-order phase transition described in II. These were obtained basically as the mean temperature between the closest arrows representing relaxations from metastable states, as indicated in Fig. 5; the error bars reported in Table I, increasing with ρ, aim to locate approximately the corresponding limit of metastability or spinodal line. More accurate methods of computing the coexistence and spinodal lines$^{(8,9)}$ are expected to give essentially the same result, while they would require prohibitive amounts of computer time in the present case, where one has to deal with the presence of transient states with several strips, anisotropic clustering above $T^*(\rho)$, and stronger finite-size effects than usual.

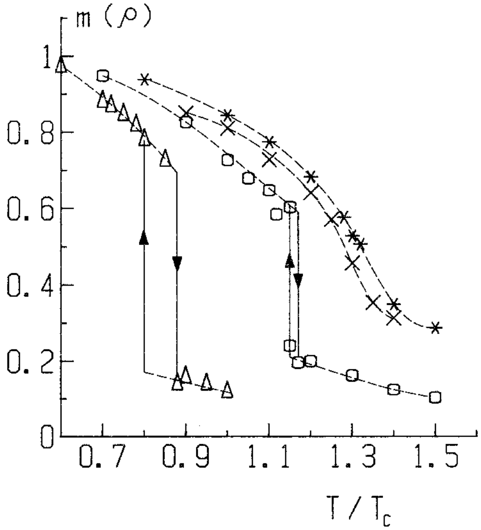

Fig. 5. The order parameter as defined by Eq. (3.1) as a function of temperature for different values of $\rho = (\triangle)\ 0.1$, $(\bigcirc)\ 0.2$, $(\times)\ 0.35$, and $(*)\ 0.5$. The vertical arrows locate the closest transitions observed between the corresponding two branches when the system is heated from zero temperature and cooled from infinite temperature, respectively.

Table I. Transition Temperature As a Function of ρ^a

ρ	T^*
0.50	1.355 ± 0.003
0.35	1.32 ± 0.02
0.20	1.16 ± 0.02
0.10	0.84 ± 0.04
0.075	0.67 ± 0.13
0.05	0.37 ± 0.18

[a] The error bars represent the location of the closest metastable states we observe during the system evolution; cf. Fig. 5.

The resulting phase diagram is shown in Fig. 6, where it is compared with the equilibrium Onsager case and with the classical mean-field result. Two facts seem to follow from Fig. 6. First, the present (pseudo-) spinodal is much closer to the coexistence curve than in the usual classical theory (see, e.g., Ref. 10). Also, the experimental data for both $m(T, \rho = 1/2)$ and $T^*(\rho)$ near T_c^* lie between the equilibrium and mean-field results, thus apparently confirming that the basic model belongs to a new universality class.

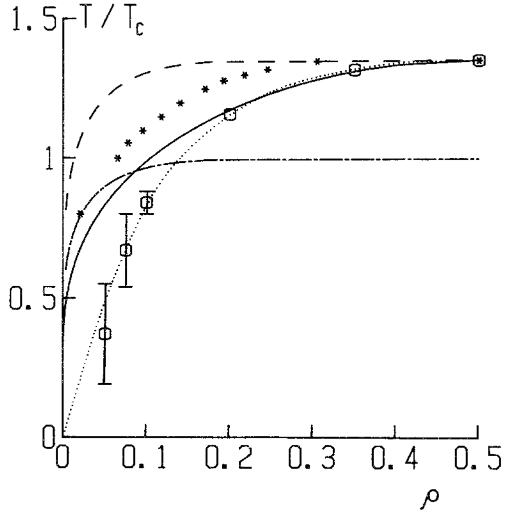

Fig. 6. A representation of the (○) transition temperatures in Table I with the corresponding "error bars" (see text) locating the limit of metastability. (—) The classical mean-field result, (- -) the equilibrium Onsager result, both normalized to $T_c^* = T^*(\rho = 1/2)$. (∗) The curve $m(T)$ for $\rho = 1/2$ described in II. (···) A guide to the eye associated with the circles; (— · —) the Onsager result.

4. ENERGY, SPECIFIC HEAT, AND STRUCTURE FUNCTION

The nature of the phase transition may also be investigated by looking at other relevant quantities; we refer to II for their precise definition. In particular, the configurational energy (Fig. 7) and the particle current in the direction of the field (Fig. 8) reveal the characteristic discontinuities, and the structure function (Table II) behaves quite anisotropically and its maximum is observed to increase very abruptly with decreasing temperature below $T^*(\rho)$.

The specific heat, which is computed here as the temperature derivative of the configurational energy by making cubic interpolations to the data, is represented in Fig. 9. This presents a clear discontinuity for $\rho \leqslant 0.2$, a behavior quite different from the case $\rho = 1/2$ (cf. Fig. 8 in II) and perhaps also differing qualitatively from the case $\rho = 0.35$.

5. COMPARISONS WITH EXPERIMENTAL OBSERVATIONS

The great interest in the properties of fast ionic or superionic conductors (FIC) during the last decade[2-4,11-13] essentially has been motivated by their promising technological applications[4]; e.g., they may reach ionic conductivities of the order of $1\ \Omega^{-1}\ \mathrm{cm}^{-1}$ well below the melting point (as compared to $10^{-8}\ \Omega^{-1}\ \mathrm{cm}^{-1}$ for the solid NaCl at 200°C). Those studies,

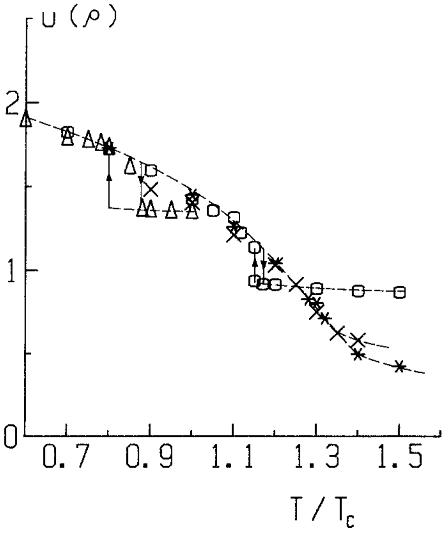

Fig. 7. Total configurational energy as a function of temperature for different values of ρ; same symbols as in Fig. 5.

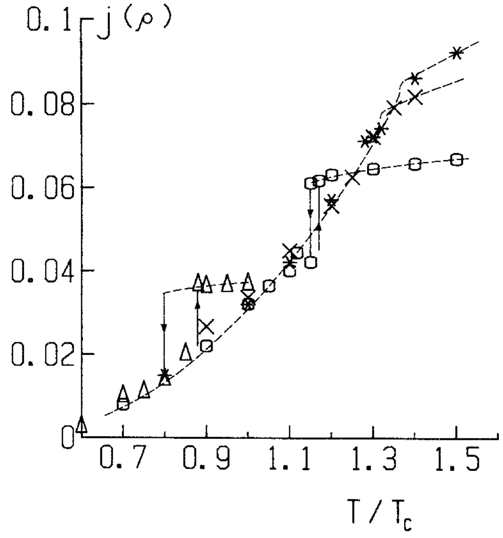

Fig. 8. Particle current in the direction of the field as a function of temperature for different values of ρ. Same symbols as in Fig. 5.

however, have also revealed a more fundamental interest of FIC; they are outstanding examples of (relatively simple) systems with stationary nonequilibrium states showing both continuous and discontinuous instabilities(1) and also relating in some way liquid and solid properties. The latter follows when one realizes that FIC typically possess at high temperatures the conductivity of some melts and the mechanical properties of some solids, and that typically (e.g., in the case of α-AgI), a type of ion (Ag*) seems to move in a liquidlike fashion through a lattice set up by another type of ion (I^-),(14) so that one has to deal in practice with the

Table II. Representative Values of the Structure Function $S(k_x, k_y=0)$ for Different Values of $k_x=(2\pi/L)\,n_x$, $n_x=1$, 2, and 3, and $L=50$

	$S(k_x, k_y=0)$				$S(k_x, k_y=0)$		
T/T_c	$n_x=1$	$n_x=2$	$n_x=3$	T/T_c	$n_x=1$	$n_x=2$	$n_x=3$
0.7	322	212	99	1.1	372	126	52
1.0	167	124	74	1.25	260	96	18
1.12	104	74	43	1.3	110	71	26
1.2	<5	<5	<5	1.35	62	28	16
1.3	<3	<3	<3	1.4	<10	<10	<10

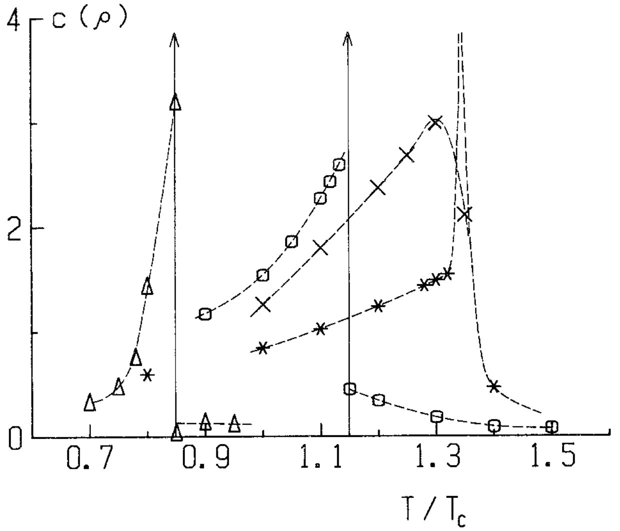

Fig. 9. The specific heat, defined as the temperature derivative of the total configurational energy, as a function of temperature for different values of ρ. Same symbols as in Fig. 5; the dashed lines are guides to the eye.

interesting phenomenon of the diffusion of a liquid through a solid. This outstanding mobility of the conducting ions (whose number is typically of the order of the Avogadro number) is usually associated with the existence of a large amount of vacant positions in the lattice, either lattice sites or interstitials,(2) this apparently causing the onset of the high-conductivity phase often to be characterized by large discontinuities. In any case, it seems clear that a large degree of disorder sets in at the (nonequilibrium) transition temperature, probably as a consequence of the "melting" of one of the sublattices, and sometimes a corresponding change of entropy was measured comparable to the one for the melting in that material.(18,19)

Such features of FIC seem certainly well mimicked by our model system, e.g., in the case $\rho \ll 1/2$. As a matter of fact, the claim that the oversimplified model captures many essential physical features of FIC is supported by the observation that quite different materials (inorganic crystals, glasses, polymers, etc.) seem to present the same basic phenomena, including the case of ice, where there was a recent report(15) of a first-order phase transition at high temperature to a state characterized by a large concentration of ionic defects allowing a high conductivity. It is true that most experiments refer to relatively small electric fields as compared to the "infinite" one in the model; however, previous studies of the model with several fields(1) seem to reveal only quantitative differences when considering the infinite-field limit, a case more suitable for a theoretical analysis, and on the other hand, the fields considered by experimentalists may be well within the saturation regime.

When making comparisons with the behavior of real materials, one should also realize that the conductivity in FIC frequently occurs as a low-dimensionality effect. For instance, the substance hollandite is known to behave as a quasi-one-dimensional conductor, where K^+ ions are compelled to move in channels,(16) and the conducting ions in $AgCrS_2$ always remain within lattice planes.(17) This suggests in particular an unusual physical relevance of the one- and two-dimensional model systems in this case. On the other hand, the fac that one- (or quasi-one-) dimensional materials undergo phase transition phenomena may indicate the existence of some mean-field effects, a fact also revealed by the analysis of the model in the preceding sections and elsewhere.(1)

The global experimental situation is in practice rather varied. That is, while the onset of a high ionic conductivity below the melting point is usually associated with typical phase transition phenomena, the reported nature of those phenomena was used to classify FIC.(2) The *type I* materials are characterized by a well-defined first-order phase transition, e.g., AgI presents a four-decade jump in the conductivity at the transition temperature. The most general behavior of the materials in this group is certainly represented very well by our model with $\rho \ll 1/2$. We do not attempt a specific comparison in this case because the experimental results are not very clear-cut, e.g., due to the presence of polymorphic transitions and hysteresis and other effects.

The materials reported as being of *type II*, on the other hand, are supposed to be characterized by a second-order phase transition, though we believe, in light of the discussion in the previous sections, that they present more generally a weak first-order transition(5) or a transient behavior such as the one shown by our model in the case $\rho = 0.35$. Actually, the materials in this group show a conductivity versus temperature curve that only reveals a change of slope at the transition temperature, either abrupt (as in $AgCrS_2$) or more gradual (as reported for PbF_2, perhaps due to experimental difficulties producing a "diffuse transition"), and the specific heat shape measured(2) in $AgCrS_2$ is also very similar to the one in Fig. 9 for the model with $\rho \approx 1/2$. In order to emphasize the close similarity between some experimental results and those in our model, we present in Fig. 10 the extrapolation for $L \to \infty$ of the current along the field directions j_x in the case of the model with $\rho = 1/2$, together with the ionic resistance for some real materials. The similarity is indeed very remarkable when one realizes that the experimental result refers to a three-dimensional situation, and that it corresponds to $\rho = 0.29$

and involves a structural change from cubic to rhombohedric.(20) The behavior of j_x for the model also compares very well in Fig. 10 with that of the ionic conductivity measured, for instance, by Hibma(21) in $AgCrS_2$; this material is indeed very comparable with the model, given that it presents a two-dimensional conduction and approximately half the accessible sites are known to be vacant,(17) so that $\rho \approx 1/2$.

There are few detailed studies of the critical properties of FIC; Refs. 5, 20 and 22 report critical behavior close to the one corresponding to the equilibrium three-dimensional Ising model. More experiments in this area would be very helpful, specially those concerning low-dimensionality materials and large external electric fields, focusing on the nature of the nonequilibrium phase transition and critical properties.

Finally, we mention that, in addition to the above types of FIC, experimentalists have reported on the existence of a *type III*, e.g., Na-β-Al_2O_3.(2) This, however, is not well represented by the model here, because the corresponding conductivity in those materials is observed to increase exponentially over a broad range of temperatures, probably reflecting that sharp cooperative effects are absent. It also seems puzzling

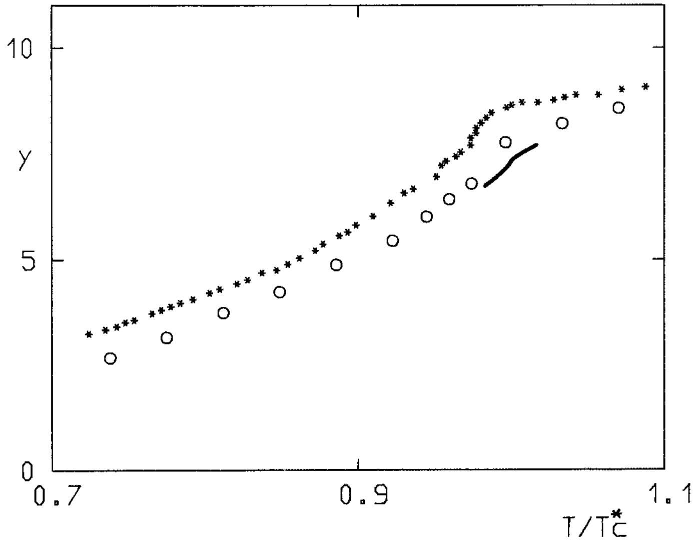

Fig. 10. The particle current along the field direction, as measured in the model when $\rho = 1/2$ by making an extrapolation to $L \to \infty$, compared with some experimental results. (○) Infinite-size model, $y = 12.2/j_x$; (*) $AgCrS_2$,(21) $y = 3(\sigma T_c^*)^{0.2}$, where σ represents the ionic conductivity in units of $(\Omega\text{-cm})^{-1}$ and $T_c^* \equiv 673$ K; (—) $NH_4Ag_4I_5$,(20) $y = 270/R$, where R represents the ionic resistance in units of ohms, and $T_c^* \equiv 198.68$ K. The units for the vertical axis are thus arbitrary.

that some real materials reported as being of types I or II apparently contain antiferromagnetic couplings, while some versions of the model with $J<0$ (instead of $J>0$ as in the present paper) show the suppression of the original antiferromagnetic phase transition when the (strong) external electric field is turned on.(1) This compels one to think that the predominant or effective interactions in those materials might be ferromagnetic-like, and it suggests as well studying the model with $J<0$.

6. CONCLUSIONS

The lattice-gas model (with periodic boundary conditions and the distinguishing feature that the particles are interpreted as positive ions interacting via a nearest neighbor attractive potential), under the influence of an external saturating electric field along one of the principal lattice directions, constitutes a good (oversimplified) model system to study the interesting properties of the so-called fast ionic conductor (FIC) materials. These properties, it should be stressed, are a stationary nonequilibrium effect: the field induces a current of particles in the system, this generating heat, which is dissipated by means of (stochastic) interactions between the ions and the involved thermal reservior at temperature T.

An extensive Monte Carlo study in two dimensions also reveals a critical point at density $\rho = 1/2$ and temperature $T_c^* > T_c$ (the equilibrium, Onsager critical temperature), while the FIC model undergoes discontinuous or first-order phase transitions for $\rho \ll \rho_c$; the discontinuities, if any, are extremely weak within the range $1/2 < \rho \lesssim 0.35$, and quite evident for $\rho \leqslant 0.2$. The segregation below, say, $T^*(\rho)$, $T^*(\rho_c) \equiv T_c^*$, is anisotropic in the sense that it produces orientated domains, namely the system asymptotically relaxes into a particle-rich strip along the field direction coexisting with a homogeneous particle-poor gas. The computer simulations showed two different kinds of intermediate states: (a) When ρ is large enough, say, for $\rho \gtrsim 0.2$, the system first segregates into a multistrip state; the number of strips and the time of escape seem to increase with system size, the latter also increasing (even diverging) with decreasing temperature. (b) Metastable states below and near the coexistence line $T^*(\rho)$ have the usual (equilibrium) features, e.g., they are nonsegregated. No doubt it would be interesting, and feasible, to attempt a dynamical description of the phase segregation processes in the FIC model following the trends familiar from nucleation and spinodal decomposition phenomena (see, e.g., Ref. 23).

Concerning the stationary (nonequilibrium) properties, the coexistence line $T^*(\rho)$ (as it occurs with the relevant critical exponents at T_c^*) is halfway between the equilibrium one by Onsager and the classical one by

Landau, both normalized to T_c^*. There is a rather well-defined spinodal line; this is a mean-field feature, but it lies closer to $T^*(\rho)$ than predicted by the classical theory and it is not so close to $T^*(\rho)$ (and is more abrupt) than observed during computer simulations of the equilibrium lattice-gas model (see, e.g., Ref. 24). It is also noticeable (Fig. 6) that $T^*(\rho) > T(\rho)$ for $\rho \gtrsim 0.15$, while $T^*(\rho) < T(\rho)$ for smaller values of ρ; $T(\rho)$ represents here the equilibrium, Onsager coexistence lines. This is a consequence of the action of the electric field: it strengthens the correlations above T_c in such a way that it produces instability within the temperature range $T_c < T < T_c^*$, while it destroys the equilibrium clusters near $T(\rho)$ for $\rho < 0.15$ when the number of particles is insufficient to form a strip.

We have also computed in the model relevant physical quantities, in addition to the order parameter, such as energies and specific heats, the structure function as it could be measured in scattering experiments, ordering susceptibilities, and particle currents. They globally confirm the above facts and, most interesting, allow us to make the first contact between the behavior of the model and the observations in FIC materials. For instance, a comparison between our data in Fig. 9 and those reported for the specific heat in real materials,(5,20,25) together with a close inspection of the comparison, as in Fig. 10, between the behavior of the currents, conductivities, and resistances,(20,21) adscribes a clear physical significance to the reported existence(2) of two types of FIC materials; *type I* would correspond to the case $\rho \lesssim 0.2$ in the model, characterized by strong discontinuities, while the materials termed *type II* seem to include both the case of a critical density with a second-order phase transition and the case $\rho_c < \rho \lesssim 0.3$ discussed before. Those comparisons also allow one to identify and confirm some other features of FIC, as described in the preceding section, even though the available experimental data refer to materials that are in principle not so comparable to our oversimplified model. Similar studies concerning more realistic models ($J < 0$, more extended interactions, etc.) and, moreover, new experimental measurements on FIC materials would be very helpful; in particular, motivated by the apparent existence of a new universality class, experimentalists should concentrate on the computation of critical indexes in the case of low-dimensionality FIC materials such as those where the ionic conductivity occurs in planes, in the presence of a saturating field.

ACKNOWLEDGMENTS

We acknowledge useful discussions with Joel L. Lebowitz, as well as valuable correspondence with Henk van Beijeren, Herbert Spohn, and

J. Krug. This work was partially supported by the U.S.–Spanish Cooperative Research Program under grant CCB-8402025 and by the CAICYT under Project PB85-0062, Spain.

REFERENCES

1. J. L. Vallés and J. Marro, *J. Stat. Phys.*, this issue, preceding paper.
2. J. B. Boyce and A. B. Huberman, *Phys. Rep.* **51**:189 (1979).
3. W. Dietrich, P. Fulde, and I. Peschel, *Adv. Phys.* **29**:527 (1980).
4. J. B. Bates, J. Wang, and N. J. Dubney, *Phys. Today* **1982**(July):46.
5. Yu. Ya. Gurevich and Yu. Kharkats, *Phys. Rep.* **139**:201 (1986).
6. K. Binder and H. Müller-Krumbhaar, *Phys. Rev. B* **9**:2328 (1974).
7. O. Penrose and J. L. Lebowitz, *J. Stat. Phys.* **3**:211 (1971); in *Fluctuation Phenomena*, E. W. Montroll and J. L. Lebowitz, eds. (North-Holland, Amsterdam, 1979).
8. M. Creutz, L. Jacobs, and C. Rebbi, *Phys. Rev. D* **20**:1915 (1979).
9. O. G. Mouritsen, *Computer Studies of Phase Transitions and Critical Phenomena* (Springer-Verlag, Berlin, 1984).
10. K. Binder, M. Kalos, J. L. Lebowitz, and J. Marro, *Adv. Colloid Interface Sci.* **10**:173 (1979).
11. S. Geller (ed.), *Solid Electrolytes* (Springer-Verlag, Berlin, 1977).
12. G. D. Mahan and W. L. Roth (eds.), *Superionic Conductors* (Plenum Press, New York, 1976).
13. M. B. Salamon (ed.), *Physics of Superionic Conductors* (Springer-Verlag, Berlin, 1979).
14. M. L. Rice, S. Strässler, and G. A. Toombs, *Phys. Rev. Lett.* **32**:596 (1974).
15. I. A. Ryzhkin, *Solid State Commun.* **56**:57 (1985).
16. H. U. Beyeler, in *Physics in One Dimension*, J. Bernasconi and T. Schneider, eds. (Springer-Verlag, Berlin, 1981).
17. P. Brüesch, T. Hibma, and W. Bührer, *Phys. Rev. B* **27**:5052 (1983).
18. W. Hayes, *Contemp. Phys.* **19**:469 (1978).
19. M. O'Keeffe and B. G. Hyde, *Phil. Mag.* **33**:219 (1976).
20. R. A. Vargas, M. B. Salamon, and C. P. Flynn, *Phys. Rev. B* **17**:269 (1978).
21. T. Hibma, *Solid State Commun.* **33**:445 (1980).
22. W. J. Pardee and G. D. Mahan, *J. Chem. Phys.* **61**:2173 (1974).
23. J. D. Gunton, M. San Miguel, and P. S. Sahni, in *Phase Transitions and Critical Phenomena*, Vol. 8, C. Domb and J. L. Lebowitz, eds. (Academic Press, London, 1983).
24. J. Marro and R. Toral, *Am. J. Phys.* **54**:1114 (1986).
25. E. Vlieg, H. W. den Hartog, and M. Winnink, *J. Phys. Chem. Solids* **47**:521 (1986).